

# DYNAMIC PHASOR MEASUREMENTS USING SUBSPACE BASED TECHNIQUES FOR SYNCHROPHASOR APPLICATIONS

P. Banerjee and S.C. Srivastava  
Indian Institute of Technology Kanpur  
Kanpur-208016, India  
param@iitk.ac.in, scs@iitk.ac.in

**Abstract** – The accuracy of the dynamic phasor estimation, utilizing steady state signal model can be greatly improved by employing subspace based techniques of spectral estimation. This paper has utilized TLS-ESPRIT and Propagator Method for this purpose and provides a comprehensive performance analysis based on Total Vector Error (TVE), frequency error and the step response. The validity of the subspace based technique has been, further, investigated through simulation of fault on 10 machine 39-bus system. The phasor estimation by the Propagator method, without eigen decomposition, has outperformed the accuracy requirement and, hence, can be considered for the dynamic phasor estimation in PMUs.

**Keywords:** *Synchrophasor, PMU, Phasor estimation, TLS-ESPRIT, MUSIC, Propagator method*

## 1 INTRODUCTION

In the recent years, monitoring and control of large interconnected power systems has become a challenging task. A steady state operating condition of the power system is perturbed by various events, like sudden addition or rejection of bulk loads, severe faults, and loss of transmission lines or generators. The occurrences of such disturbances cause the entire power system to drift from equilibrium and may lead to instability, if remedial actions are not taken in time. Hence, effective and fast monitoring of the system dynamic states is desirable, which has become possible with the advent of synchrophasor based measurement system [1]. The three phase voltage phasors at all the buses in a power system form the states, which provide complete observability of the system. The synchrophasor based Wide Area Monitoring System (WAMS) can provide voltage phasors at buses, which are located geographically apart. Typically, WAMS consists of Phasor Measurement Units (PMUs). A Global Positioning System (GPS) clock is used to generate a reference phasor and the instantaneous bus voltage measurements are analyzed at PMUs to define corresponding voltage vector with respect to this reference phasor. The time stamp in the phasor data enables the real time monitoring and control of the power system. The instantaneous values of the voltages are sampled over a short time interval and the Discrete Fourier Transform (DFT) [1] based algorithm has been, generally, used to compute the amplitude and phase of the voltages over the data sample window. The steady state operation of the power system is well visualized by voltage phasor complying IEEE Standard 37.118-2005 [2], which defines standards and performance requirements of the synchro-

phasor measurements in terms of Total Vector Error (TVE within 1%), and tests to ensure these limits as well as the communication data protocol. However, under a dynamic condition, the static signal model, which is used to derive the voltage phasor using the DFT algorithm, fails to report the actual phasor value due to drifting of the system frequency to off nominal value, phase jumps and amplitude change. Hence, standards for dynamic phasor measurements are under development [3]. The phasor reporting rates for the dynamic phasor estimation have to be extended in multiples and submultiples of the system nominal frequency ( $f_{nom}$ ), ranging from 30 phasor per second for a 60Hz system to  $2f_{nom}$  for effectively capturing the dynamic scenario under transients.

During recent years, several versions of the DFT algorithms have been developed considering the dynamic signal model. Yang et al. [4] have proposed a robust frequency estimation technique, but it takes only one non integral harmonic into consideration. Demodulation based frequency estimation algorithm has been suggested in [5], which uses filters of 4 cycles, resulting into delay of 2 cycles and frequency error greater than 0.4 Hz. Dynamic phasor measurement has to comply with the high speed estimation requirement. A half cycle dynamic phasor estimation has been proposed in [6]. This utilizes a lookup table and orthogonal finite impulse response filters, which also suffer from non flat top mid band gain and higher side lobes. These characteristics of the FIR filters result in spectral leakage and inaccurate phasor measurements. Phasor estimation, by incorporating frequency deviation in the signal model, has been attempted by Wang et al. [7], which shows good phase and frequency estimation. Phasors are fitted to second order Taylor polynomial by Serna [8] using least square approach, and the frequency response of the second order model is studied.

In this paper, phasors under power system dynamic conditions are estimated by using subspace based techniques. The subspace based techniques are well known high frequency resolution techniques for spectral estimation in signal processing. Various algorithms available in this class of spectral estimation are MUSIC (Multiple Signal Classification), TLS-ESPRIT (Total Least Square-Estimation of Signal Parameters via Rotational Invariance Techniques) [9] and Propagator Method (PM) [10]. The Subspace based method for spectral estimation involves formation of correlation matrix from the signal samples of measurement window and, then, solving an eigen value problem. Frequency of the

fundamental signal component is estimated by using TLS-ESPRIT and PM. By solving the signal model with known frequency, amplitude of the fundamental signal component is estimated. The Phase estimation by TLS-ESPRIT method is based on the eigen decomposition of the correlation matrix of the reference signal samples and, instead of using the first shift of the signal eigen vector, the eigen vector of the correlation matrix of the reference signal is employed. Similarly the correlation matrix of the reference is also used for calculating the phase difference by PM. The performance of the dynamic phasor estimation by TLS-ESPRIT and PM is evaluated on the basis of the Total Vector Error (TVE). The test cases attempted for the performance evaluation are sinusoidal signals with off-nominal system frequency, introducing frequency ramp, step change in phase and amplitude of a synthetically generated signal. The phasor estimation by subspace based technique is, further, validated by introducing fault in New England (NE) 39-bus system.

## 2 BRIEF DESCRIPTION OF TLS-ESPRIT AND PROPAGATOR METHODS

The fundamental voltage in a power system can be expressed as real sinusoidal signal, of the form given below.

$$s(t) = X_{m1} \cos(2\pi f_0 t + \phi) \quad (1)$$

where,  $X_{m1}$  is the peak value,  $\phi$  is the initial phase,  $f_0$  is the fundamental frequency. The phasor value of the above signal is  $S = (X_{m1}/\sqrt{2})\angle\phi$

Under a disturbance, the amplitude and phase no longer remain constant, but become functions of time. The dynamic model of the voltage for phasor estimation can be expressed as a band pass signal, with amplitude and phase dependent on time, of the form.

$$s(t) = X_{m1}(t) \cos(2\pi f_0 t + \phi(t)) \quad (2)$$

The dynamic phasor at a time instant  $t$  can be defined as  $S(t) = (X_{m1}(t)/\sqrt{2})\angle\phi(t)$

The voltage signals are sampled at fixed interval and the sampled values are accumulated to form a vector of data size  $M$ . Similarly the reference waveform is also generated and synchronously sampled to form a reference vector of same length. The discrete signal model of the reference and the voltage signals can be expressed as given below.

$$\begin{aligned} x(n) &= s(n-D) \\ y(n) &= s(n) + z(n), \quad n = 0, 1, \dots, M-1 \end{aligned} \quad (3)$$

$$\text{where, } s(n) = \sum_{i=1}^p a_i e^{j\omega_i n} \quad (4)$$

The  $s(n)$  is modeled by sum of  $p$  complex sinusoids, in which amplitudes  $a_i$  are unknown complex value constants with corresponding normalized frequency  $\omega_i$  in rad/sec and  $D$  is the sample delay reflected as phase. The factor  $p$  is pre estimated by the user. The complex white Gaussian noise for the data signal is denoted

by  $z(n)$ , while the internal generated reference signal is assumed to be noise less.

### 2.1 TLS-ESPRIT method

The real signal can be expressed as a pair of complex exponentials, one having frequency negative of the other. Hence, the data vector of length  $M$  can be expressed as

$$\begin{bmatrix} y(n) \\ y(n+1) \\ \vdots \\ y(n+M-1) \end{bmatrix} = \sum_{k=1}^p \begin{bmatrix} s_k(n) \\ s_k(n+1) \\ \vdots \\ s_k(n+M-1) \end{bmatrix} + \begin{bmatrix} z(n) \\ z(n+1) \\ \vdots \\ z(n+M-1) \end{bmatrix} \quad (5)$$

For  $K$  real harmonic components, the signal can be represented as a linear combination of  $p = 2K$  exponential basis as follows:

$$s_k(n) = \alpha_k e^{jn\omega_k} \begin{bmatrix} 1 \\ e^{j\omega_k} \\ \vdots \\ e^{j(p-1)\omega_k} \end{bmatrix} \quad (6)$$

Substituting (6) in (5) provides

$$y(n) = \mathbf{A}\mathbf{S} + \mathbf{z}(n) \quad (7)$$

where,  $\mathbf{S} = [\hat{a}_1, \hat{a}_2, \dots, \hat{a}_p]^T$ ,  $\hat{a}_k = \alpha_k e^{jn\omega_k}$  and

$$\mathbf{A} = \begin{bmatrix} 1 & 1 & \dots & 1 \\ e^{j\omega_1} & e^{j\omega_2} & \dots & e^{j\omega_p} \\ \vdots & \vdots & \ddots & \vdots \\ e^{j(M-1)\omega_1} & e^{j(M-1)\omega_2} & \dots & e^{j(M-1)\omega_p} \end{bmatrix}$$

The correlation matrix, formed from the sampled data, has a rotational invariance property of the signal subspaces spanned by two displaced data vectors. This characteristic is exploited by the Estimation of Signal Parameters via Rotational Invariance Techniques (ESPRIT) [11]. For a sinusoidal model, the time shift can be modeled as a phase shift. Hence, the time shifted data vector is expressed as

$$[y(n+1), \dots, y(n+M)]^T = \mathbf{A}\mathbf{S}\mathbf{\Gamma} + \mathbf{z} \quad (8)$$

where,  $\mathbf{\Gamma} = \text{diag}\{e^{j\omega_1}, e^{j\omega_2}, \dots, e^{j\omega_p}\}$  is the phase shift matrix, which is a rotation on a unit circle.

The actual auto correlation matrix is defined as follows, where  $E(\bullet)$  denotes the expectation

$$\mathbf{R}_{yy} = E(y(n)y^H(n)) = \mathbf{A}\mathbf{R}_s\mathbf{A}^H + \sigma^2\mathbf{I} \quad (10)$$

where  $(\bullet)^H$  denote the Hermitian transpose,  $\mathbf{R}_s$  is the covariance matrix of the signal and  $\sigma^2$  is the variance of the Gaussian noise. The covariance matrix from the data vectors is factorized into symmetric orthogonal basis by Singular Value Decomposition (SVD). The eigen vectors corresponding to the significant  $p$  eigen values form the signal space and the remaining eigen vectors are basis of the noise subspace. The first  $(M-1)$  rows of

the signal subspace are formed as  $\mathbf{U}_1$  and one row shifted  $M-1$  rows of the signal subspace is formed as  $\mathbf{U}_2$  of the total  $M$  rows of the signal subspace. Finally, the total least square estimation of the rotation of the two subspaces is obtained, which is denoted by  $\hat{\Psi}$ , as given in [12]. The eigen values of  $\hat{\Psi}$  are computed, which are expressed as a diagonal matrix, previously denoted by  $\Gamma$ . The imaginary part of the natural logarithm of  $\Gamma$  divided by the sampling time gives the frequency in rad/sec. The calculation of phase shift of the signal with respect to the reference is obtained by replacing the  $\mathbf{U}_2$  matrix of the signal subspace by first  $M-1$  rows of the signal subspace of the covariance matrix formed from the reference vector.

## 2.2 Propagator method

The frequency estimation by propagator method is a subspace based technique which does not involve eigen decomposition of cross correlation matrix of the received signal. The data vector of the signal of length  $M$  is arranged in  $M/2 \times M/2$  Hankel matrix as follows [13].

$$\mathbf{Y} = \begin{bmatrix} y(0) & y(1) & \dots & y(M/2-1) \\ y(1) & y(2) & \dots & y(M/2) \\ \vdots & \vdots & \ddots & \vdots \\ y(M/2-1) & y(M/2) & \dots & y(M-1) \end{bmatrix} \quad (11)$$

From the signal model, the Hankel matrix can be written as  $\mathbf{Y} = [\mathbf{r}(0) \ \mathbf{r}(1) \ \dots \ \mathbf{r}(M/2-1)]$ . The  $i^{\text{th}}$  column of  $\mathbf{Y}$  is given by

$$\mathbf{r}(i) = \mathbf{A}_L(\omega)(\boldsymbol{\varphi}(\omega))^i \mathbf{a} + \mathbf{u}_i \quad i = 0, 1, \dots, M/2-1 \quad (12)$$

where,

$$\mathbf{A}_L = \begin{bmatrix} 1 & 1 & \dots & 1 \\ e^{j\omega_1} & e^{j\omega_2} & \dots & e^{j\omega_p} \\ \vdots & \vdots & \ddots & \vdots \\ e^{j(M/2-1)\omega_1} & e^{j(M/2-1)\omega_2} & \dots & e^{j(M/2-1)\omega_p} \end{bmatrix}$$

and,  $\boldsymbol{\varphi}(\omega) = \text{diag}\{e^{j\omega_1} e^{j\omega_2} \dots e^{j\omega_p}\}$ ,  $\mathbf{a} = [a_1, a_2, \dots, a_p]^T$

The  $\omega_p$  are the  $2K$  frequencies in the real signal and  $\mathbf{a}$  is the complex amplitude vector. The matrix  $\mathbf{A}_L$  is partitioned into two matrices  $\mathbf{A}_{L1}$  and  $\mathbf{A}_{L2}$  having dimensions as  $p \times p$  and  $(M/2 - p) \times p$ , respectively. The propagator matrix  $\mathbf{P}$  is related to  $\mathbf{A}_{L1}$  and  $\mathbf{A}_{L2}$  as

$$\mathbf{P}^H \mathbf{A}_{L1}(\omega) = \mathbf{A}_{L2}(\omega) \quad (13)$$

where,  $(\bullet)^H$  denote the Hermitian transpose.

The Hankel matrix, when partitioned by  $p$  rows and  $(M/2 - p)$  rows denoted by  $\mathbf{Y}_1$  and  $\mathbf{Y}_2$ , does not actually satisfy the propagator equation. Hence, a least square estimate of the propagator is calculated from the partitioned Hankel matrix as follows.

$$\hat{\mathbf{P}} = \arg \min \left\| \mathbf{Y}_2 - \hat{\mathbf{P}}^H \mathbf{Y}_1 \right\|^2 = (\mathbf{Y}_1 \mathbf{Y}_1^H)^{-1} \mathbf{Y}_1 \mathbf{Y}_2^H \quad (14)$$

The estimated matrix  $\hat{\mathbf{P}}$  is augmented by negative identity matrix of dimension  $(M/2 - p) \times (M/2 - p)$ , which is denoted by  $\hat{\mathbf{E}}$  to make it full rank.

$$\hat{\mathbf{E}} = \begin{bmatrix} \hat{\mathbf{P}} \\ -\mathbf{I} \end{bmatrix} \quad (15)$$

Ideally, the basis of  $\hat{\mathbf{E}}$  is orthonormal to array response matrix  $\mathbf{A}_L$ . But due to the noise, the orthonormal projection matrix  $\mathbf{Q}$  is calculated from the estimated  $\hat{\mathbf{E}}$  as  $\mathbf{Q} = \hat{\mathbf{E}}(\hat{\mathbf{E}}^H \hat{\mathbf{E}})^{-1} \hat{\mathbf{E}}^H$  (16)

Now MUSIC algorithm [14] can be applied to calculate the basis of  $\mathbf{A}_L$ . The Multiple Signal Classification (MUSIC) is a noise space based method for spectral estimation. MUSIC finds the basis vector, which is orthogonal to the noise subspace by finding the peaks of the inverse product of the basis vectors and the noise subspace.

$$\hat{\omega}_p = \arg \max \frac{1}{\mathbf{A}_L^H \mathbf{Q} \mathbf{A}_L} \quad (17)$$

In MUSIC algorithm, the resolution of the frequency can be provided by the user. The resolution should be carefully selected considering slow changes in the system frequency. The frequency resolution considered in this work is  $2e-04$  Hz.

The phase of the data signal with respect to the reference signal can be calculated by the propagator method, which is discussed below.

The data vectors of both the signals and the reference of length  $M$  are employed to construct individual  $M/2 \times M/2$  Hankel matrices, which are combined as follows  $\mathbf{Z} = \begin{bmatrix} \mathbf{X} \\ \mathbf{Y} \end{bmatrix}$  (18)

The discrete signal model reduces the expression of  $\mathbf{X}$  as

$$\mathbf{X} = [\mathbf{A}_L \boldsymbol{\Omega} \mathbf{a} \ \mathbf{A}_L \boldsymbol{\Omega} \boldsymbol{\varphi} \mathbf{a} \ \dots \ \mathbf{A}_L \boldsymbol{\Omega} \boldsymbol{\varphi}^{M/2-1} \mathbf{a}] \quad (19)$$

where,  $\boldsymbol{\Omega} = \text{diag}\{e^{-jD\omega_1} e^{-jD\omega_2} \dots e^{-jD\omega_p}\}$

The Propagator matrix is obtained by partitioning the combined Hankel matrix  $\mathbf{Z}$  into  $\mathbf{Z}_1$  and  $\mathbf{Z}_2$ , having dimensions  $p \times pM/2$  and  $(M - p) \times pM/2$ , respectively

$$\hat{\mathbf{P}} = (\mathbf{Z}_1 \mathbf{Z}_1^H)^{-1} \mathbf{Z}_1 \mathbf{Z}_2^H \quad (20)$$

The obtained Propagator matrix  $\hat{\mathbf{P}}$  is partitioned into three sub matrices,  $\hat{\mathbf{P}}_1$  and  $\hat{\mathbf{P}}_3$ , each having dimension  $(M/2 - p) \times p$ , and  $\hat{\mathbf{P}}_2$  having dimension  $p \times p$ .

The phase angle is the argument of the eigen values of  $\hat{\mathbf{P}}_2$ , which corresponds to the  $p$  complex sinusoid.

However, in the model of the data signal considered, its  $p$  frequencies are taken same as that of the reference signal. This assumption is not true, when the system frequency drifts. Hence, off-nominal frequency compensation has been done for the phase, which is a function of the calculated instantaneous frequency obtained from the PM.

### 3 PERFORMANCE EVALUATION

The dynamic phasor estimation of the voltage signal consists of correct measurement of the amplitude, phase, frequency and rate of change of frequency during steady state and transient conditions. The accuracy of the estimated phasor has been measured by its TVE, which is defined as follows.

$$TVE = \sqrt{\frac{(X_r(n) - X_r)^2 + (X_i(n) - X_i)^2}{X_r^2 + X_i^2}} \quad (21)$$

where  $X_r(n)$  and  $X_i(n)$  are the real and imaginary components of the measured value of the phasor, given by the algorithm utilized, and  $X_r$  and  $X_i$  are the corresponding theoretical true values of the input signal at the time of the measurement. Other than TVE, frequency error is also evaluated from the instantaneous estimates of the frequency by TLS-ESPRIT and PM. The Frequency Error (FE) is defined as the absolute value of the difference between its theoretical value and the estimated/measured value, in Hz.

$$FE = |f_{\text{true}} - f_{\text{measured}}| \quad (22)$$

The measured and true values are for the same instant of time, which, in practice, can be picked up from the timetag of the estimated phasors. This is achieved by using proper group delay compensation. The group delay is a time lag for the actual occurrence of the event and the time when the algorithm generates the response. Any inconsistency in the reporting time causes different errors with different algorithms due to inconsistency in the reporting time. In this work, the absolute time of the center of the measurement window is considered as the reporting time. This is justified because the event occurring within the measurement window may be considered as an averaging effect on the data within the window.

The second harmonic content of the voltage signal is very less or negligible. Hence, half cycle estimation of the voltage signal can be safely implemented for synchrophasor applications. The performance of the phasor estimation by the TLS-ESPRIT and the PM are evaluated on mathematically generated signals and, then, on signal data acquired from PSCAD/EMTDC [15] simulation on the NE 39-bus test system. Various events are incorporated in the mathematically generated signals, like off nominal frequency, phase shift, frequency ramp and step change in the amplitude and the phase. The test signals are sampled at a rate of 8.3 kHz and a data vector, of length 70, is created, which corresponds to approximately half cycle of the voltage signal. The internal reference signal, generated by using the ticks of the high precision GPS clock, is also synchronously sampled with the same sampling rate and accumulated as the reference vector of the same length as the signal data vector. The sliding window type data vector updating is implemented, which means that the most recent sample shifts the entire vector, thus, discarding the most obsolete data. As the present method is employed for dynamic phasor estimation, high reporting rate is desirable. The PMU, having reporting rates less

than 10/sec, may not be required to comply with the dynamic test requirement. With the increasing communication bandwidth and reduced latency, the technology has become mature enough for higher reporting rates, as high as 100/sec and 120/sec for the 50 and 60Hz systems, respectively. In this work, reporting rates of 120/sec has been considered for the 60 Hz systems.

#### 3.1 Off-nominal frequency test

The system frequency may be at off-nominal value, when load generation imbalance occurs. Figure 1 shows the phase estimated with the DFT, TLS-ESPRIT and the PM methods for a sinusoidal signal with frequency of 62Hz. The nominal system frequency is 60Hz.

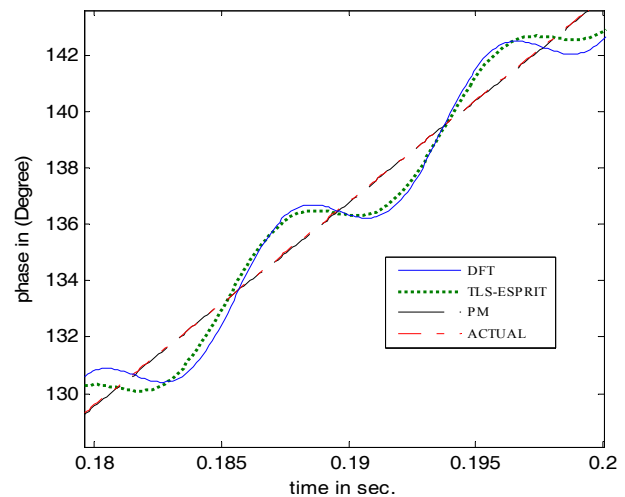
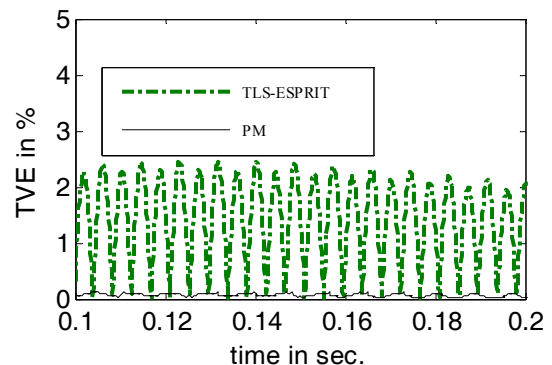
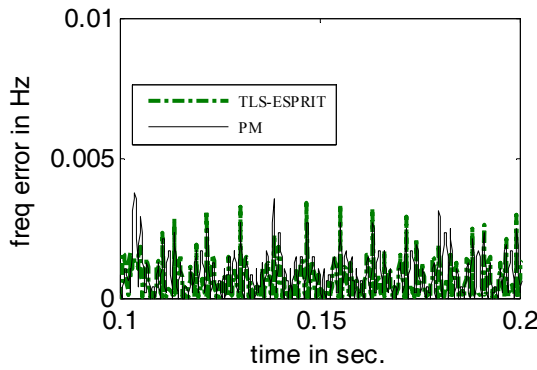


Figure 1: Phase estimated for system frequency of 62 Hz

The large error in the calculated phase value in Figure 1 with the DFT is because the DFT algorithm does not accommodate off-nominal frequency and, hence, the phase and amplitude oscillates significantly, while there are no amplitude oscillations in case of TLS-ESPRIT. Keeping view of this, the DFT has not been considered for comparison in the subsequent work. The plot of TVE with the TLS-ESPRIT and PM is shown in Figure 2. The phase computation by the TLS-ESPRIT has oscillations, because the change in the system frequency does not satisfy the shift invariance, unless the phase shift is compensated by the actual frequency deviation while considering the signal subspace of the data correlation matrix. The phase plot of the PM practically overlaps with the actual phase value in Figure 1. The TVE with the PM is below 0.2% as can be observed from the Figure 2.



**Figure 2:** TVE for the system frequency of 58Hz



**Figure 3:** FE in Hz for the system frequency of 62Hz

As shown in Figure 3, the frequency error for both the subspace based methods is less than 0.005Hz. Thus, both the TLS-ESPRIT and the PM can estimate off-nominal frequency accurately.

### 3.2 Initial Phase shift with frequency offset

The estimation of the phase offset when frequency is off-nominal has been identified as a test criteria. Figure 4 shows the TVE for a phase shift of  $90^\circ$ , when system frequency is 59.75Hz. The maximum frequency drift for measuring the phase shift can be restricted to 0.25Hz. The maximum TVE observed in case of the PM for this test is less than 0.1%.

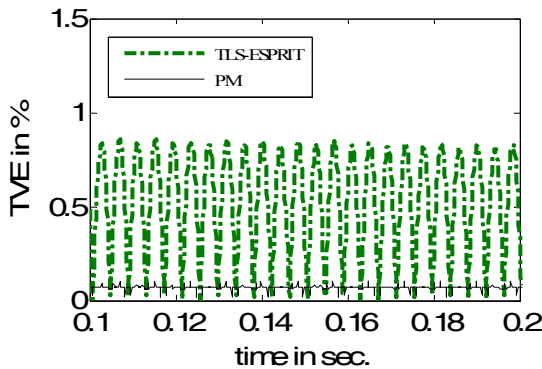


**Figure 4:** Phase shift of  $90^\circ$  with system frequency of 59.75Hz.

### 3.3 Frequency ramp test

The acceleration of the rotor causes the system frequency to change from its nominal value. The signal model for such a scenario can be expressed as a ramp in the frequency parameter.

$$\begin{aligned} X_a &= X_m \cos(\omega_0 t + \pi R_f t^2) \\ X_b &= X_m \cos(\omega_0 t - 2\pi/3 + \pi R_f t^2) \\ X_c &= X_m \cos(\omega_0 t + 2\pi/3 + \pi R_f t^2) \end{aligned} \quad (22)$$

where,  $R_f = 2$  Hz/sec is the frequency ramp rate considered. The ramp was initiated at 0.1 sec. and continued till 0.5 sec. It is also desired that the error calculation may exclude the first 2 samples from the inception of the frequency ramp. The steady state frequency,

before and after the ramp, are 59.8Hz and 59Hz, respectively.

The plot of the frequency is shown in Figure 5. Figure 6 shows the error in the frequency for the ramp test, which lies well below 0.01Hz, with both the TLS-ESPRIT and PM.

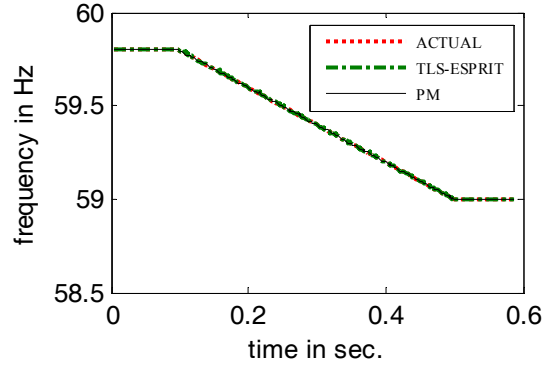


**Figure 5:** Frequency ramp of 2Hz/s

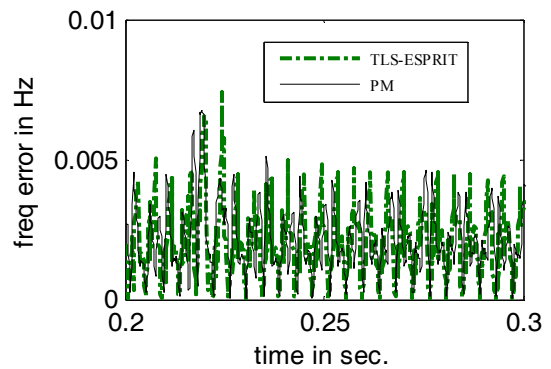


**Figure 6:** Frequency error for ramp of 2Hz/s

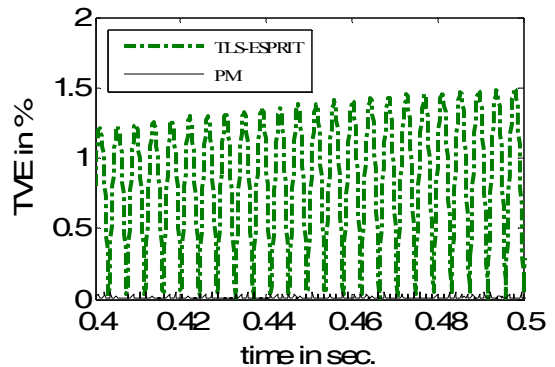


**Figure 7:** TVE for frequency ramp 2Hz/sec

The TVE with the PM reaches a maximum value of 0.05% in the whole run, as shown in Figure 7.

### 3.4 Amplitude and phase step response

The step response is a phenomenon of instantaneous change of the system states from one value to the other. The performance under the step response is evaluated on the basis of the response time, response delay and maximum overshoot. The definition of the parameters, for evaluating a step response, is shown in Figure 8.

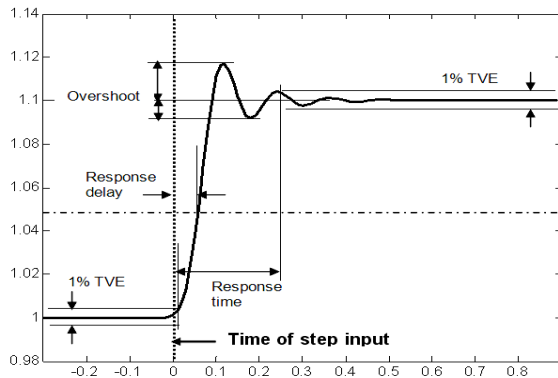


**Figure 8:** Definition of various parameters for evaluating step response.

The step change in the amplitude is considered as the 10% of its nominal value and that in the phase as  $10^\circ$ . The actual and the estimated values of the response for the step change in amplitude, with the two methods, are shown in Figure 9.

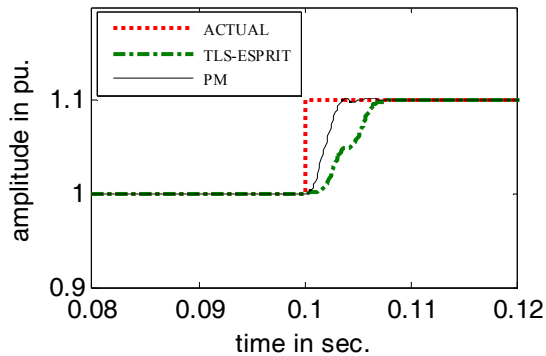


**Figure 9:** Response for step change in amplitude

The response time for the PM is 0.0044 sec and the TLS-ESPRIT method is 0.0076 sec, which is well below 1/Phasor reporting frequency. The maximum overshoot with the PM is 3% and there is practically no overshoot with the TLS-ESPRIT method. The step response for phase change is shown in Figure 10. The response time for the PM is 0.0044 sec and that with the TLS-ESPRIT is 0.0082 sec, which is also below 1/Phasor reporting frequency. The maximum overshoot with the PM is 6.6% and there is practically no overshoot with the TLS-ESPRIT method.

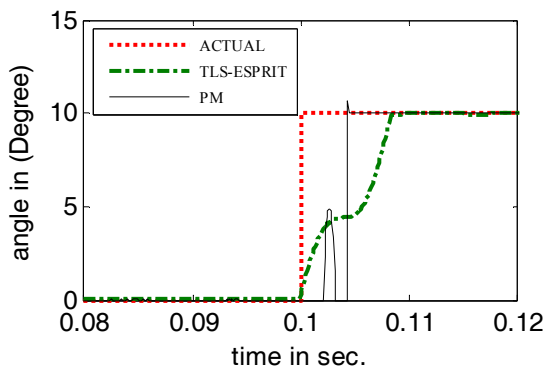


**Figure 10:** Response for step change in phase.

### 3.5 Fault case in NE 39-bus system

The subspace based algorithms, verified on the test signals, have given satisfactory results in terms of the TVE, the frequency error and the response time. The error in the phase estimation by the TLS-ESPRIT method increases as the system frequency becomes more off nominal. But it provides equally efficient frequency estimation. The Propagator method scans the system frequency from 54Hz to 66Hz, as a result the precision depends on the resolution in which the frequency range is divided. The validity of the TLS-ESPRIT and the PM are further tested by placing a PMU at one of the buses in the NE 39-bus system [16] and simulations obtained by the PSCAD/EMTDC. The PMU was assumed to be placed at bus 2. A 3 phase fault is applied on a line connecting buses 2-19 at 0.5 sec and cleared at 0.15 sec. The time of the fault and the fault impedance have been chosen such that the power oscillations of substantial magnitude are not generated. The acquired data is processed by both the TLS-ESPRIT and the PM algorithms. The phase voltage plot is shown in Figure 11. Before the fault, the peak of the voltage is approximately 277kV, which is estimated correctly by both the TLS-ESPRIT and the PM. The recovery of the bus voltage, after the fault is cleared, can be seen in Figure 12. The phase jumps are also tracked by both the TLS-ESPRIT and the PM. The effectiveness of the subspace based methods can also be visualized by the frequency estimates, which show minor fluctuation with the PM in Figure 14.

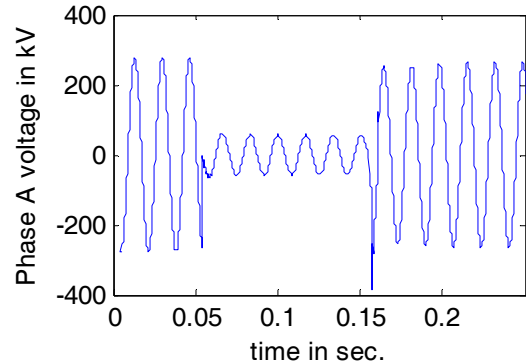


**Figure 11:** Phase voltage in kV

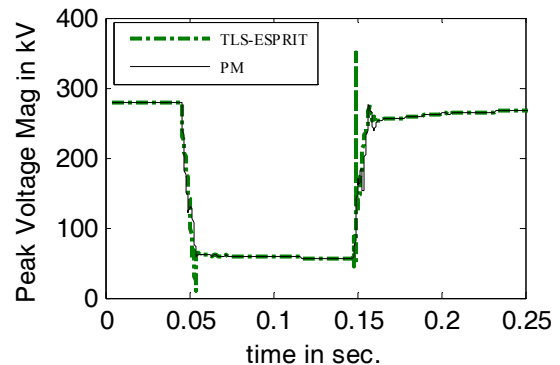


**Figure 12:** Amplitude estimates in kV (NE 39-bus system)

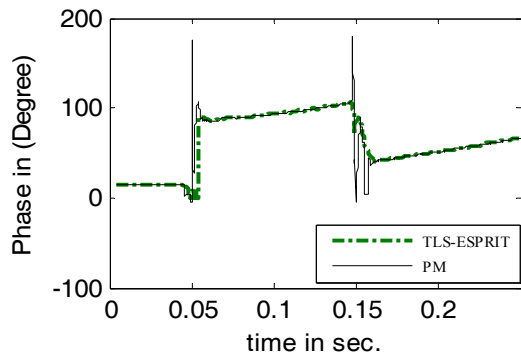


Figure 13: Angle estimates in (Deg) (NE 39-bus system)

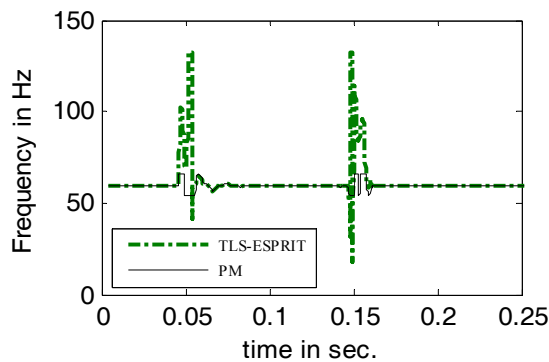


Figure 14: Frequency estimates in Hz (NE 39-bus system)

#### 4 CONCLUSION

This paper proposes the application of TLS-ESPRIT and Propagator methods for achieving accurate dynamic phasor estimates. The effectiveness of the two subspace based methods for dynamic phasor estimation has been studied under various test cases, which include the off-nominal system frequency, phase shift in the presence of frequency offset, frequency ramp test and step response for amplitude and phase. The PM has been found to be highly accurate in terms of TVE, FE and step input response. The performance of the subspace based algorithm, using half cycle data samples, has been tested through simulation of a fault in NE 39-bus system using PSCAD/EMTDC, which shows satisfactory result of the dynamic phasor estimation.

#### ACKNOWLEDGEMENT

Authors gratefully acknowledges the partial financial support provided by Department of Science and technology, New Delhi under project no. DST/EE/20100258, for carrying out this research work.

#### REFERENCES

[1] A. G. Phadke and J. S. Thorp, "Synchronized Phasor Measurements and Their Applications", New-York, Springer, 2008, ISBN 978-0-387-76535-8, pp 17-20  
 [2] IEEE Std. C37.118-2005 Standard for Synchrophasors for Power Systems, 2006.

[3] PMU System Testing and Calibration Guide: North American Synchrophasor Initiative (NASPI). Dec. 30, 2007. [Online]. <http://www.naspi.org>  
 [4] Jun-Zhe Yang and Chih-Wen Liu, "A precise calculation of power system frequency", IEEE Transactions on Power Delivery, vol.16, no.3, pp.361-366, Jul 2001.  
 [5] I. Kamwa, M. Leclerc and D. McNabb, "Performance of demodulation-based frequency measurement algorithms used in typical PMUs", IEEE Transactions on Power Delivery, vol.19, no.2, pp. 505- 514, April 2004.  
 [6] T.S Sidhu, Xudong Zhang and V. Balamourougan, "A new half-cycle phasor estimation algorithm", IEEE Transactions on Power Delivery, vol.20, no.2, pp. 1299- 1305, April 2005.  
 [7] Maohai Wang and Yuanzhang Sun, "A practical, precise method for frequency tracking and phasor estimation", IEEE Transactions on Power Delivery, vol.19, no.4, pp. 1547- 1552, Oct. 2004.  
 [8] J.A. de la Serna, "Dynamic Phasor Estimates for Power System Oscillations", IEEE Transactions on Instrumentation and Measurement, vol.56, no.5, pp.1648-1657, Oct. 2007.  
 [9] D. G. Manolakis, V. K. Ingle and S. M. Kogon, "Statistical and adaptive signal processing: spectral estimation, signal modeling, adaptive filtering, and array processing", Boston, Artech House, 2005, ISBN 1-58053-610-7.  
 [10] Sylvie Marcos, Alain Marsal and Messaoud Benidir, "The propagator method for source bearing estimation", Signal Processing, vol. 42, Issue 2, pp. 121-138, March 1995,  
 [11] R. Roy and T. Kailath, "ESPRIT-estimation of signal parameters via rotational invariance techniques", IEEE Transactions on Acoustics, Speech and Signal Processing, vol.37, no.7, pp.984-995, Jul 1989  
 [12] Gene H. Golub and Charles F. Van Loan "Matrix Computations" (3rd ed.) The Johns Hopkins University Press, pp 596, (1996).  
 [13] M. M. Qasaymeh, Hiren Gami, Nizar Tayem, M. E. Sawan, and Ravi Pendse, "Joint Time Delay and Frequency Estimation Without Eigen-Decomposition", IEEE Signal Processing Letters, vol.16, no.5, pp.422-425, May 2009.  
 [14] R. O. Schmidt, "Multiple emitter location and signal parameter estimation", IEEE Transactions on Antennas and Propagation, vol. AP-34, no. 3, pp. 276-280, Mar. 1986.  
 [15] PSCAD/EMTDC, Manitoba HVDC Research Center, [www.pscad.com](http://www.pscad.com).  
 [16] K.R. Padiyar, "Power System Dynamics Stability and Control", Bangalore, Interline publishing private Ltd., 1996.